A preliminary study on introduction of a magnetic tracking sensor for bronchoscope navigation system

Kazuyoshi Ishitani*
Graduate School of Information Science, Nagoya University

Daisuke Deguchi†
Graduate School of Information Science, Nagoya University

Takayuki Kitasaka‡
Graduate School of Information Science, Nagoya University

Kensaku Mori§
Graduate School of Information Science, Nagoya University

Yasuhito Suenaga¶
Graduate School of Information Science, Nagoya University

Hirotsugu Takabatake
Minami-sanjo Hospital

Masaki Mori
Sapporo-Kosei general Hospital

Hiroshi Natori
Keiwakai Nishioka Hospital

Abstract

In this paper, we investigate the adaptability of a miniature-sized magnetic positional sensor in a bronchoscope navigation system. A key component of a bronchoscope navigation system is a magnetic positional sensor that can capture the position of the tip of a bronchoscope. However, in a clinical environment, the accuracy of a magnetic sensor decreases due to the magnetic field distortion caused by ferromagnetic materials around the sensor. Therefore, we introduce a method to correct the sensor's outputs by utilizing a magnetic tracking sensor and an optical tracking sensor. In this method, a sensor's output is corrected by using a higher-order polynomial whose coefficients are computed from 5000 points measured by the optical and magnetic sensors. This measurement is performed prior to bronchoscopy. The experimental results show that the correction method can reduce distortion errors from 53.3 mm to 3.5 mm or below. We also confirmed that sufficiently accurate bronchoscope camera motion could be obtained for the bronchoscope navigation system.

CR Categories: J.3 [Computer Applications]: Life and Medical Sciences—Medical Information Systems; I.4.8 [Computing Methodologies]: Image Processing and Computer Vision—Tracking

Keywords: bronchoscope, navigation, magnetic tracking sensor, optical tracking sensor, motion tracking

1 Introduction

A bronchoscope is a very important tool for observing and diagnosing the inside of the bronchus. A medical doctor inserts it into the bronchus by operating a controller at the tail of the tube while watching a TV monitor displaying the views captured by a tiny camera installed at the tip of the bronchoscope. To reach a desired branch, the physician should insert the bronchoscope in such a way that passes several branches. However, the doctor can become easily disoriented because the anatomical structures of the bronchus are very complicated and the bronchus exhibits individual differences in its branching patterns. Therefore, it is necessary to develop a system that guides a physician to a location where biopsy is performed. Another important function is the visualization of anatomical structures beyond the bronchus walls based on preoperative CT images and their synchronized display with real bronchoscopic images.

Virtual bronchoscopy (VB) is now widely used to observe the inside a human body based on three-dimensional (3-D) CT images [1, 2, 3, 4, 5, 6, 7]. The user of a virtual bronchoscopy system (VBS) can freely perform a fly-through inside a target organ with a pointing device such as a mouse. A VB has several advantages over a real bronchoscope (RB), including (a) observation from any viewpoint or view direction, (b) quantitative measurement, and (c) visualization of anatomical structures beyond organ walls by semi-transparent rendering. If we could combine real and virtual bronchoscopes in bronchoscopy, it would be possible to construct a guidance or navigation system for bronchoscopy.

A bronchoscope navigation system provides guidance information obtained from preoperative CT images. Prior to bronchoscopy, we take a 3-D CT image of a patient. The navigation system continuously tracks the camera motion and provides navigation information obtained by fusing virtual and real bronchoscopic views (Fig. 1). Also, the location and orientation of the tip of a bronchoscope are displayed on the slice images throughout the examination. One of the most important functions of the bronchoscope navigation system is continuous tracking of a bronchoscope's tip. If we could obtain motion information of the tip, it would be possible to present the path to a desired position where biopsy is performed or to present some quantitative measurements.

Positional sensors are used for tracking a camera's or surgical instrument's position in an image-guided surgery system [8, 9, 10, 11]. In the case of a rigid endoscope, sensing points consisting of infrared LEDs or reflection spheres are attached at its tail (exposed to the exterior of the patient), and an optical (OP) tracking system located in a surgical or examination room senses their positions optically. In the case of a flexible endoscope, such as a bronchoscope, it is impossible to estimate the position and orientation of the tip from positions of markers attached at the tail by the OP tracking system due to the flexibility of the bronchoscope. Introduction of a tracking system using the electromagnetic field (EM tracker) is a good solution for this case. Recently, miniature-sized EM tracking systems have been commercial-

*e-mail: kishitani@suenaga.m.is.nagoya-u.ac.jp
†e-mail: ddeguchi@suenaga.m.is.nagoya-u.ac.jp
‡e-mail: kitasaka@is.nagoya-u.ac.jp
§e-mail: kensaku@is.nagoya-u.ac.jp
¶e-mail: suenaga@is.nagoya-u.ac.jp

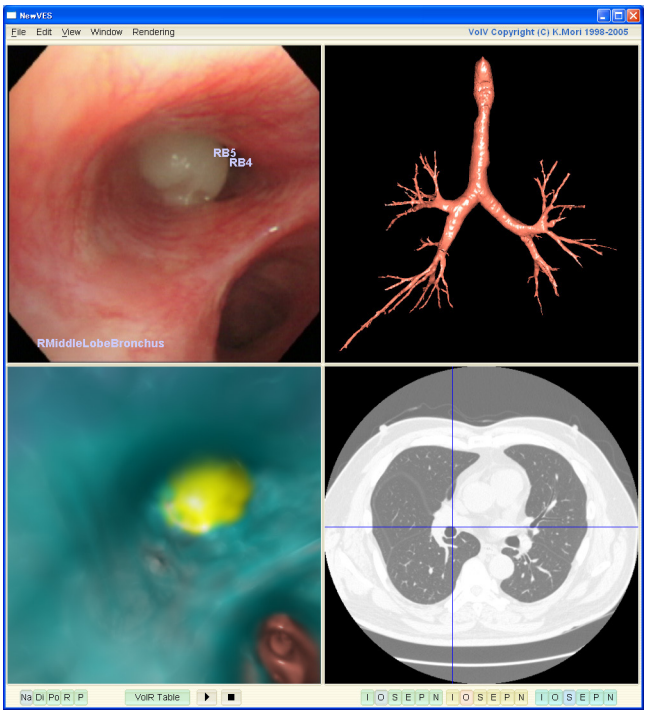

Figure 1: Snapshot of bronchoscope navigation system. There are four kinds of images in this system in separate windows: (upper left) real bronchoscopic video, (upper right) outside view of bronchus, (lower left) virtual bronchoscopic view, and (lower right) slice image. Live bronchoscopic video is played in real bronchoscopic window. A tracheal tumor is observed in RB view. Position currently being observed is overlaid on outside view of bronchus. In virtual bronchoscopic view window, anatomical structures existing beyond bronchus wall are visualized by utilizing semi-translucent display. Bronchus wall in this figure is semi-translucent light-blue, tumor is yellow. Current position of bronchoscope is marked with cross cursor in the slice window. These windows are synchronized to movement of real bronchoscope.

ized by several companies. These sensors can be inserted into bronchoscopes through working channels. The common problem of EM tracking systems is the degradation of tracking accuracy due to magnetic field distortion caused by ferromagnetic materials located around the sensing points. These ferromagnetic materials distort the magnetic field so that the EM tracker outputs unreliable sensing results. To overcome this problem, we try to correct magnetic field distortion by using both the OP and EM tracking systems. Sensing errors caused by magnetic field distortion are corrected by outputs of the OP tracking system. Several research groups are also tackling this problem [12, 13, 14, 15, 16]. Nakada et al. [14] proposed a method for correcting sensor output by using an OP tracking system for laparoscopic surgery navigation system. In this method, several points are sensed by both the OP and EM sensors to correct EM sensor's outputs. They developed a freehand acquisition tool for easy measurement. By moving this tool over a surgical table, the positions of a set of 3-D points are measured by the OP and EM tracker. A higher-order polynomial for correcting the EM tracker's outputs is calculated by using the outputs of the OP tracker as a gold standard. During an actual surgical procedure, the outputs of the EM tracker are compensated by using the

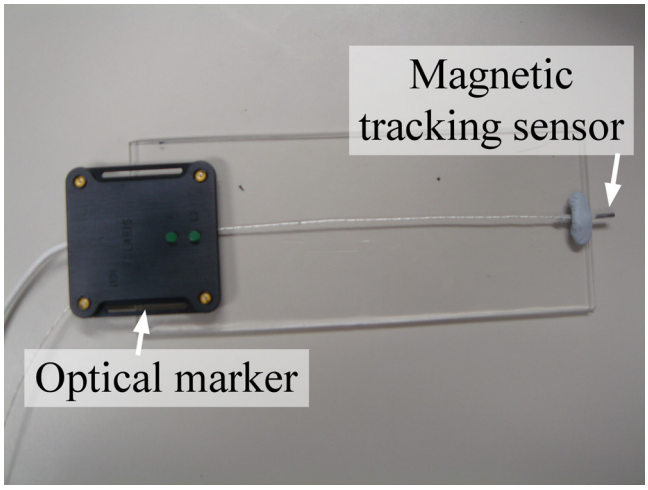

Figure 2: Distortion measurement tool.

polynomial. Chung et al. [15] reported the freehand calibration method of optical and electromagnetic trackers for bronchoscope navigation. They tested the correction method in an office and a hospital bronchoscopy environment. However, they used a 5-DOF (five degrees of freedom) sensor for obtaining the position and orientation of the tip of the bronchoscope. Furthermore, they did not consider the operating table, which is the largest metal object in the bronchoscopy examination environment.

In this paper, we discuss the effectiveness of the correction method proposed by Nakada et al. in a bronchoscopy navigation system and the stability of the method in the presence of an operating table used in a bronchoscopy examination room. In the bronchoscopy environment, the operating table is one of the major causes of magnetic field distortion. Therefore, it is important to test the stability of the correction method prior to implementation in an actual bronchoscope navigation system using the EM tracker.

2 Methodology

2.1 Materials

In the experiments we conducted, the MicroBIRD[1] (Ascension Technology Corporation, Burlington, VT, USA) sensor is used as the EM tracker for acquiring the position and orientation of the tip of a bronchoscope. This EM tracker consists of three parts: (a) a system board, (b) a magnetic field generator, and (c) sensing coils. The diameter of the sensing coil is quite small (1.8 mm in coil diameter, 8.4 mm in length). The sensing coil can be easily inserted into a working channel of a typical bronchoscope. Also, this electromagnetic position sensor covers a large enough area (up to 500 mm^3) for bronchoscopy. This EM tracker provides 6-DoF outputs (three for translation and three for rotation). It is possible to directly measure 3D position and orientation. To correct the output of the EM tracker, we used the Polaris[2] (Northern Digital Inc., Waterloo, Ontario, Canada) sensor as an optical position sensor. To acquire the outputs of both sensors, a tool for sensing positions (Fig. 2) is introduced. This tool has two sensors, the EM tracker sensor

[1] http://www.ascension-tech.com/
[2] http://www.ndigital.com/

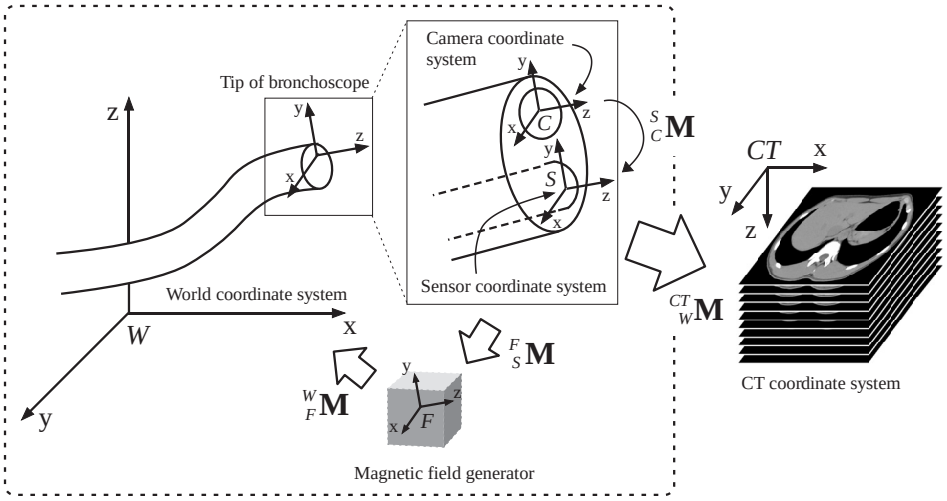

Figure 3: Relationships between sensor and CT coordinate systems.

and the OP tracker sensor. To calibrate this tool, we use another passive-type sensor for the OP tracker, and the tip of the EM tracker sensor is measured by this sensor. In our experiments, we move the tool slowly and freely above the operating table to obtain sensing ouputs.

2.2 Coordinate systems

To generate a VB image corresponding to an RB image, it is necessary to compute the transformation matrix that transforms the sensor coordinate system to the CT coordinate system. Figure 3 illustrates relationships between the sensor and CT coordinate systems. As shown in Fig. 3, the dynamic reference frame (DRF) defined by the sensor attached to the patient is considered the world coordinate system. From the relationships shown in Fig. 3, the camera coordinate $\boldsymbol{p}_C$ is transformed to the CT coordinate $\boldsymbol{p}_{CT}$ as

$$
\begin{aligned}
\boldsymbol{p}_{CT} &= {}^{CT}_{W}\mathbf{M}\,{}^{W}_{F}\mathbf{M}\,{}^{F}_{S}\mathbf{M}^{k}\,{}^{S}_{C}\mathbf{M}\,\boldsymbol{p}_C \qquad (1)\\
&= {}^{CT}_{W}\mathbf{M}\,{}^{W}_{S}\mathbf{M}^{k}\,{}^{S}_{C}\mathbf{M}\,\boldsymbol{p}_C\\
&= {}^{CT}_{W}\mathbf{M}\begin{pmatrix} {}^{W}_{S}\mathbf{R}^{k} & {}^{W}\boldsymbol{t}^{k}_{S} \\ \mathbf{0}^{T} & 1 \end{pmatrix}{}^{S}_{C}\mathbf{M}\,\boldsymbol{p}_C\\
&= {}^{CT}_{C}\mathbf{M}\,\boldsymbol{p}_C\\
&= \begin{pmatrix} {}^{CT}_{C}\mathbf{R} & {}^{CT}\boldsymbol{t}_C \\ \mathbf{0}^{T} & 1 \end{pmatrix}\boldsymbol{p}_C
\end{aligned}
$$

where ${}^{CT}_{W}\mathbf{M}$ is the transformation matrix between the world coordinate and CT coordinate and ${}^{W}_{S}\mathbf{M}^{k}$ is the sensor output represented by the world coordinate system at the k-th frame that consists of the rotational motion ${}^{W}_{S}\mathbf{R}^{k}$ and translational motion ${}^{W}\boldsymbol{t}^{k}_{S}$. The sensor output is obtained as the coordinate represented in the coordinate system of the magnetic field generator, and then it is converted to the world coordinate system by multiplying with ${}^{W}_{F}\mathbf{M}$. ${}^{S}_{C}\mathbf{M}$ represents the relationship between the tip of the bronchoscope camera and the tip of the sensor. By obtaining the transformation matrix ${}^{CT}_{C}\mathbf{M}$, which consists of rotation matrix ${}^{CT}_{C}\mathbf{R}$ and translation vector ${}^{CT}\boldsymbol{t}_C$, it is possible to generate a VB image that corresponds to the current RB camera position and orientation.

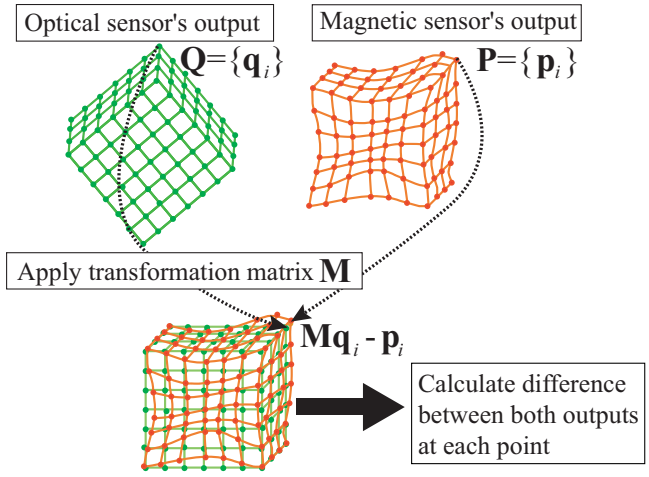

Figure 4: Method for calculating tracking error at each point.

In Eq. (1), ${}^{CT}_{W}\mathbf{M}$ and ${}^{S}_{C}\mathbf{M}$ are calculated in prior to bronchoscopy, and they are used for bronchoscope tracking. When the sensor is attached at the tip of bronchoscope, the transformation matrix ${}^{S}_{C}\mathbf{M}$ is calculated. The matrix ${}^{CT}_{W}\mathbf{M}$ is calculated using the coordinates of N fiducial points between a CT image and a real subject. To compute ${}^{CT}_{W}\mathbf{M}$, at least three corresponding point-pairs are required. If the coordinates of N ($\geq$ 3) corresponding point-pairs are obtained, ${}^{CT}_{W}\mathbf{M}$ is calculated as a closed-form solution to the least-squares problem [17].

2.3 Correction of the sensor output

In a bronchoscope operating environment, the sensor's output ${}^{W}\boldsymbol{t}^{k}_{S}$ is easily affected by objects made of ferromagnetic materials, such as an operating table, located in the operating room. By correcting the output of the EM tracker, it is possible to obtain a reliable bronchoscope position. This section describes a detailed method for correcting the output of the position sensor.

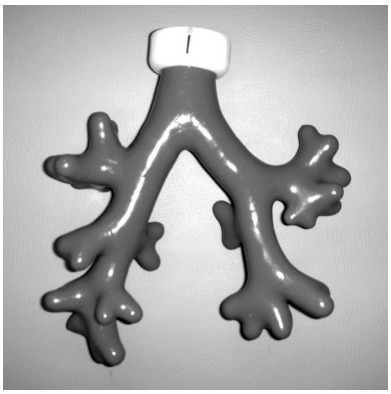

Figure 5: Example of a bronchus phantom model.

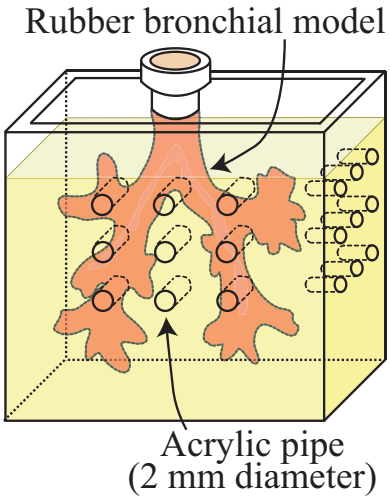

Figure 6: Layout of inserted acrylic pipes. The phantom was fixed in epoxy resin inside a plastic box, and 24 acrylic pipes were inserted.

To correct the output of the EM tracker, both sensors' outputs $\mathbf{P} = \{\boldsymbol{p}_i\}$ and $\mathbf{Q} = \{\boldsymbol{q}_i\}$ $(i = 1, \ldots, N)$ are measured using the sensing tool shown in Fig. 2. After this operation, the rigid transformation matrix $\mathbf{M}$ from the coordinate system of the optical position sensor to the magnetic position sensor can be computed using $\mathbf{P}$ and $\mathbf{Q}$ by the method shown in [17]. In an ideal case, where no distortion by metal materials is observed, we can assume that

$$\|\mathbf{M}\boldsymbol{q}_i - \boldsymbol{p}_i\| \simeq 0. \tag{2}$$

In a conventional bronchoscope examination environment, however, Eq. (2) may not be satisfied due to magnetic field distortion. We assume that this error is caused only by magnetic field distortion. We also assume that errors can be approximated by the n-th order polynomial. From these assumptions, the error function is described as

$$f(\boldsymbol{c}^x, \boldsymbol{c}^y, \boldsymbol{c}^z, \boldsymbol{p}) = \mathbf{M}\boldsymbol{q}_i - \boldsymbol{p}_i, \tag{3}$$

where $\boldsymbol{c}^x$, $\boldsymbol{c}^y$, and $\boldsymbol{c}^z$ are coefficients of a polynomial, and $\boldsymbol{p}$ is the position of the tracker output. If f is obtained, $\boldsymbol{p}$ is corrected to $\hat{\boldsymbol{p}}$ as

$$\hat{\boldsymbol{p}} = \boldsymbol{p} + f(\boldsymbol{c}^x, \boldsymbol{c}^y, \boldsymbol{c}^z, \boldsymbol{p}_i). \tag{4}$$

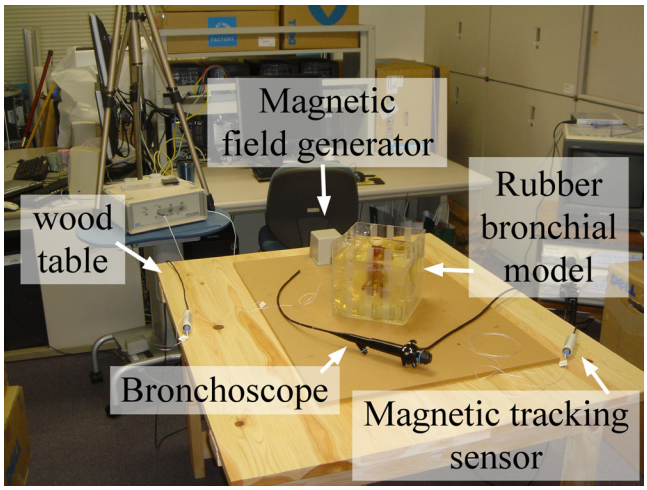

(a) free environment from ferromagnetic objects

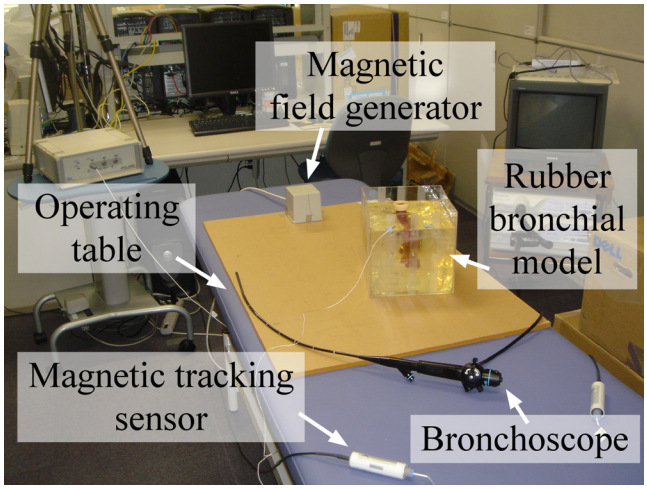

(b) bronchoscope operating environment

Figure 7: Experimental environment.

Usually, f is computed as minimizing the following equation.

$$Err = \frac{1}{N}\sum_{i=1}^{N} \|\hat{\boldsymbol{p}}_i - \boldsymbol{q}_i\|^2 . \tag{5}$$

From Eq. (4), we can rewrite Eq. (1) as follows.

$$\boldsymbol{p}_{CT} = {}^{CT}_{W}\mathbf{M} \begin{pmatrix} {}^{W}_{S}\mathbf{R} & {}^{W}\hat{\boldsymbol{t}}_S \\ \mathbf{0}^T & 1 \end{pmatrix} {}^{S}_{C}\mathbf{M}\,\boldsymbol{p}_C, \tag{6}$$

$${}^{W}\hat{\boldsymbol{t}}_S = {}^{W}\boldsymbol{t}_S + f(\boldsymbol{c}^x, \boldsymbol{c}^y, \boldsymbol{c}^z, \boldsymbol{p}_i). \tag{7}$$

3 Experiments

We applied the proposed method to the rubber bronchial phantom shown in Fig. 5. As shown in Fig. 6, the phantom was fixed in epoxy resin inside a plastic box, and 24 acrylic pipes (2 mm in diameter) were inserted into the box. These acrylic pipes were used as fiducials for calculating ${}^{CT}_{W}\mathbf{M}$ in the experiments. Prior to the experiments, we took a 3-D CT image of the phantom and manually identified the tips

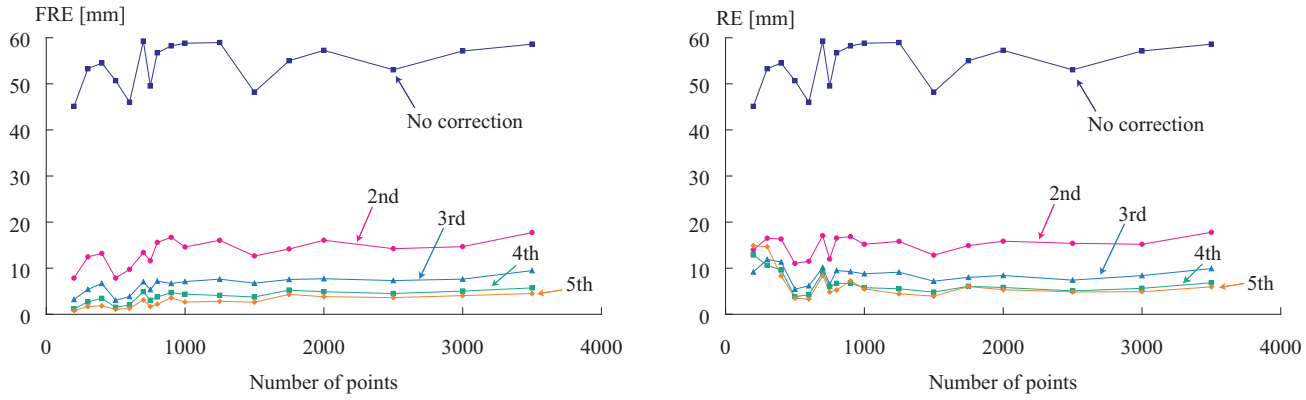

(a) FRE (b) RE

Figure 8: Results of distortion correction in an environment similar to a bronchoscope operating room (on operating table).

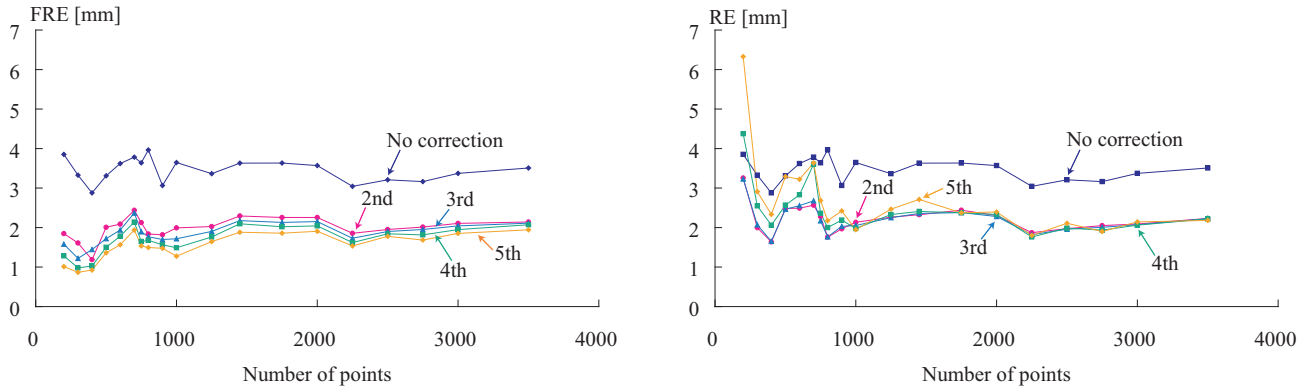

(a) FRE (b) RE

Figure 9: Results of distortion correction in an ideal environment (on wooden table).

of the acrylic pipes on the CT image. The image acquisition parameters of the CT image were 512×512 pixels, 341 slices, 0.684 mm in pixel spacing, and 0.5 mm in image spacing. To evaluate the performance of the position sensor, its outputs were measured in two kinds of environments shown in Fig. 7. Figure 7(a) is an ideal environment because there is no metal material within 1 meter from the magnetic field generator. The table is completely made of wood. Figure 7(b) shows an environment similar to a bronchoscope operating room. Since the phantom does not move during experiments, we assume that ${}^{W}_{F}\mathbf{M}$ is an identity matrix.

To test the stability of the correction method, we calculated fiducial registration error (FRE) and registration error (RE) using positions sensed by the OP and EM trackers. These errors were calculated by

$$Err = \frac{1}{N}\sum_{i=1}^{N} \|\hat{\boldsymbol{p}}_i - \boldsymbol{q}_i\| \,. \tag{8}$$

In this experiment, we used 2nd-, 3rd-, 4th- and 5th-order polynomials for correcting positions sensed by the EM tracker. Figures 8 and 9 show the results of FRE and RE by changing the number of measured positions.

Moreover, the correction method was applied to a bronchoscope navigation system. In this experiment, the bronchial phantom was placed on the operating table. The distance between the magnetic field generator and the phantom was about 300 mm. To correct the tracker's output, we measured 5000 positions with the OP and EM trackers. The measured positions were used for calculating the coefficients of Eq. (3). Figure 10 shows the results of bronchoscope tracking.

4 Discussion

As seen in Fig. 8, a large amount of measurement error (about 50 mm) was confirmed in the case no correction is employed when the position sensor was located on the operating table. From this result, it is difficult to use the EM tracker for bronchoscope navigation without correction. However, the proposed method using a 2nd-order polynomial significantly reduced measurement error to about 10 mm. Moreover, further reduction of measurement error could be achieved by using higher-order polynomials. In the case of a 4th-order polynomial, the measurement error was reduced to less than 4 mm. This result shows that higher-order polynomials are useful for correcting the EM tracker's output when distortion of the magnetic field is large. This result is a little bit worse than the result reported by Chung [15].

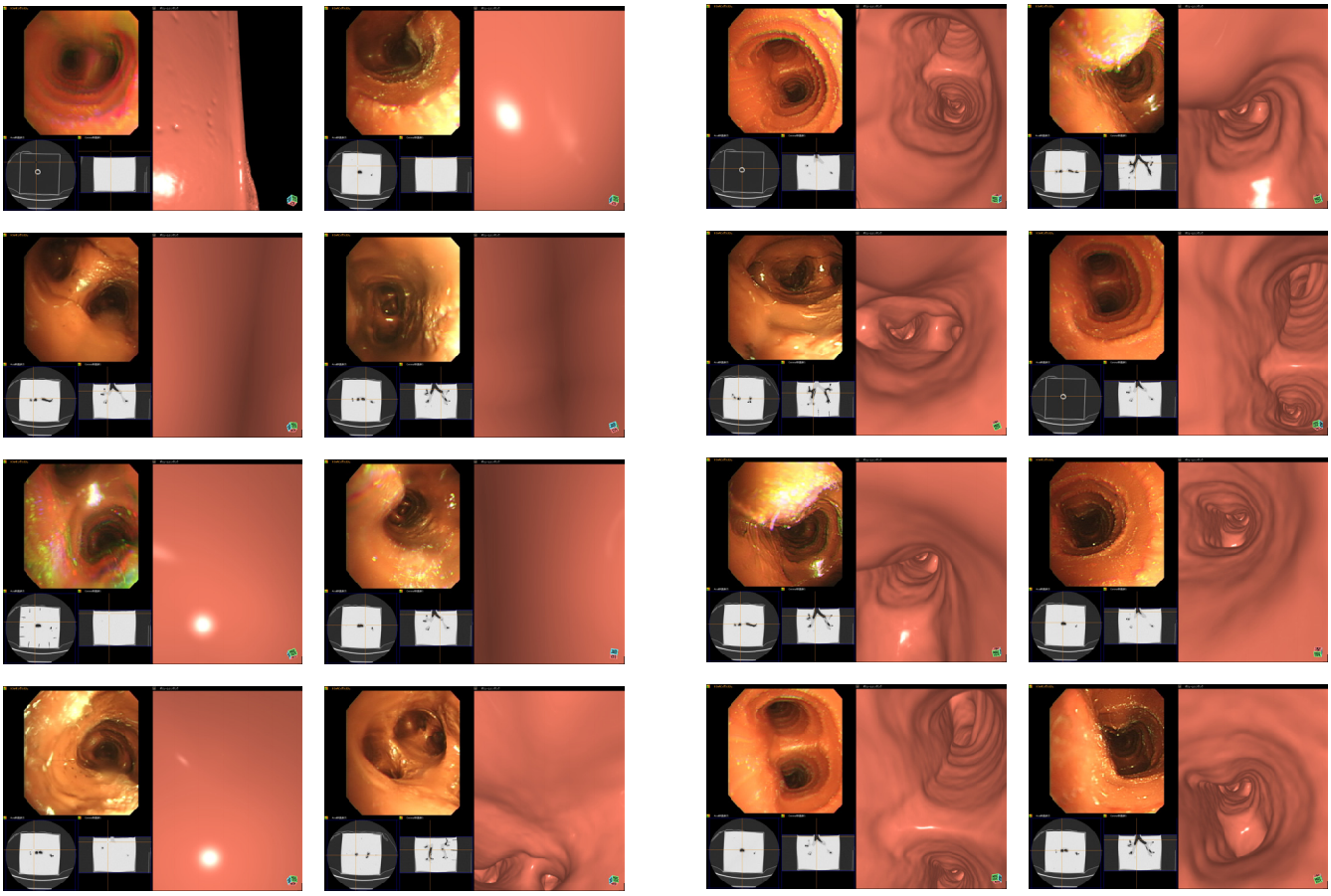

(a) without correction (b) with correction

Figure 10: Results of bronchoscope motion tracking. In each image, endoscopic view of left side is real bronchoscopic images. Right side view is a virtual bronchoscopic image generated from sensor-s outputs.

Since the distance between the magnetic field generator and the operating table was too close, distortion of the magnetic field was larger than in the case of Chung.

In the case of the ideal environment shown in Fig. 7(a), the proposed method could reduce the measurement error to 2 mm (Fig. 9). This is because the output of the position sensor was not affected by ferromagnetic objects. The EM tracker could output more accurate positions than those of distorted cases. This result is almost the same as the case of Chung. Also, it is necessary to measure the magnetic field distortion caused by other medical instruments in a real clinical environment. Even when we used 4th- or 5th-order polynomials, measurement errors were still larger than 1 mm. Since the proposed method assumed that distortion caused by objects made of ferromagnetic materials exist uniformly, the proposed method could not correct the distortion only existing in a part of the measurement space. To overcome this problem, it is necessary to divide the measurement space into sub-spaces and correct the distortion by each divided sub-space.

Figure 10 shows the results of the bronchoscope tracking in the environment shown in Fig. 7(b). In the case of no correction (Figure 10(a)), the output of the position sensor was strongly affected by metal materials such as the operating table, and the bronchoscope tracking failed. In particular, the output of the position sensor was incorrect when the bronchoscope was close to the operating table. As seen in Figure 10(b), when correction was applied, it was possible to track the bronchoscope even if it was located very close to the operating table or other ferromagnetic materials.

In this paper, we tried to correct only the positions of the EM tracker's output. However, orientation outputs of the EM tracker were also affected by ferromagnetic materials. Therefore, we could not obtain correct orientations of the bronchoscope even if the proposed method was applied (Fig. 10). To acquire accurate orientation of the bronchoscope, it is necessary to develop a method for correcting the EM tracker's orientation outputs.

5 Conclusion

This paper proposed a method for correcting the output of the position sensor for bronchoscope navigation. To employ an EM tracker for bronchoscope navigation, we applied the correction method to the outputs of the EM tracker using an OP tracker. Only positions of the EM tracker's output were corrected, and orientations were not taken into account for correction. To measure the accuracy of the correction method, we constructed two kinds of environments: (a) an ideal environment and (b) a bronchoscope operating environment. We applied our method to a rubber bronchial phantom. We found from the experimental results that the

bronchoscope tracking using 4th- or 5th- order polynomials could track the bronchoscope correctly even if the outputs of the EM tracker were affected by ferromagnetic materials. Future work includes (a) development of a method for correcting orientations of the sensor's output and (b) development of a method for compensating sensor drift caused by breathing motion.

Acknowledgements

Parts of this research were supported by a Grant-in-Aid for Scientific Research from the Ministry of Education, the 21st century COE program, a Grant-in-Aid for Scientific Research from the Japan Society for Promotion of Science, and a Grant-in-Aid for Cancer Research from the Ministry of Health and Welfare of the Japanese Government. We are also supported by the Kayamori Foundation of Informational Science Advancement.

References

[1] D. J. Vining, R. Y. Shitrin, E. F. Haponik, K. Liu, and R. H. Choplin, "Virtual Bronchoscopy," Radiology, 193 (P), Supplement to Radiology (RSNA Scientific Program), p. 261, 1994.

[2] B. Geiger and R. Kikinis, "Simulation of Endoscopy," Computer Vision, Virtual Reality and Robotics in Medicine, LNCS 905, Springer, pp. 277–281, 1995.

[3] G. Rubin, C. Beaulieu, V. Argiro, H. Ringl, A. Norbash, J. Feller, M. Dake, R. Jeffrey, and S. Napel, "Perspective volume rendering of CT and MR images: Applications for endoscopic imaging," Radiology, Vol. 199, pp. 321–330, 1996.

[4] K. Mori, A. Urano, J. Hasegawa, J. Toriwaki, H. Anno, and K. Katada, "Virtualized endoscope system –an application of virtual reality technology to diagnostic aid–," IEICE Trans. Inf. & Syst., Vol. E79–D, No. 6, pp. 809–819, 1996.

[5] L. Hong, S. Muraki, A. Kaufman, D. Bartz, and T. He, "Virtual voyage: interactive navigation in the human colon," Computer Graphics, pp. 27–34, 1997.

[6] P. Rogalla, J. Terwisscha van Scheltinga, and B. Hamm, eds., "Virtual endoscopy and related 3D techniques," Springer, Berlin, 2001.

[7] D. Caramella and C. Bartolozzi, eds., "3D Image Processing –Techniques and Clinical Application–," Springer, Berlin, 2002.

[8] H. Fuchs, A. State, E. D. Pisano, W. F. Garrett, G. Hirota, M. Livingston, M. C. Whitton, and S. M. Pizer, "Toward performing ultrasound guided needle biopsies from within a head-mounted display," Lecture Notes in Computer Science, Visualization in Biomedical Computing, Hamburg, Vol. 1131, pp. 591–600, 1996.

[9] Y. Sato, M. Nakamoto, Y. Tamaki, T. Sasama, I. Sakita, Y. Nakajima, M. Monden, and S. Tamura, "Image Guidance of Breast Cancer Surgery Using 3-D Ultrasound Images and Augmented Reality Visualization," IEEE Transactions on Medical Imaging, Vol. 17, No. 5, pp. 681–693, 1998.

[10] A. Carrillo, J. L. Duerk, J. S. Lewin, and D. L. Wilson, "Semiautomatic 3-D Image Registration as Applied to Interventional MRI Liver Cancer Treatment," IEEE Transactions on Medical Imaging, Vol. 19, No. 3, pp.175–185, 2000.

[11] P. J. Edwards, A. P. King, C. R. Maurer, Jr., D.A. de Cunha, D. J. Hawkes, D. L. G. Hill, R. P. Gaston, M. R. Fenlon, A. Jusczyzck, A. J. Strong, C. L. Chandler, and M. J. Gleeson, "Design and Evaluation of a System for Microscope-Assisted Guided Interventions (MAGI)," IEEE Transactions on Medical Imaging, Vol. 19, No. 11, pp. 1082–1093, 2000.

[12] W. Birkfellner, F. Watzinger, F. Wanschitz, R. Ewers, and H. Bergmann, "Calibration of Tracking Systems in a Surgical Environment," IEEE Transactions on Medical Imaging, Vol. 17, No. 5, pp. 737–742, 1998.

[13] M. Ikits, J. D. Brederson, C. D. Hansen, and J. M. Hollerbach, "An Improved Calibration Framework for Electromagnetic Tracking Devices," Proceedings of the Virtual Reality 2001, LNCS 2879, pp. 285–293, 2001.

[14] K. Nakada, M. Nakamoto, Y. Sato, K. Konishi, M. Hashizume, and S. Tamura, "A Rapid Method for Magnetic Tracker Calibration Using a Magneto-Optic Hybrid Tracker," Proceedings of 6th International Conference of Medical Image Computing and Computer Assisted Intervention (MICCAI 2003), LNCS 2879, pp. 285–293, 2003.

[15] A. J. Chung, P. J. Edwards, F. Deligianni, and G. Yang, "Freehand Cocalibration of Optical and Electromagnetic Trackers for Navigated Bronchoscopy," Proceedings of International Workshop on Medical Imaging and Augmented Reality (MIAR 2004), LNCS 3150, pp. 320–328, 2004.

[16] G. S. Fischer and R. H. Taylor, "Electromagnetic Tracker Measurement Error Simulation and Tool Design," Proceedings of 8th International Conference of Medical Image Computing and Computer Assisted Intervention (MICCAI 2005), LNCS 3750, pp. 73–80, 2005.

[17] B. K. P. Horn, "Closed-form solution of absolute orientation using unit quaternions," Journal of the Optical Society of America A, Vol. 4, pp. 629–642, 1987